

Chaotic Behavior and Subharmonic Bifurcations for the Duffing-van Der Pol Oscillator*

Hong Li^{1,†}, Lilin Ma² and Wenjing Zhu³

Abstract Chaotic behavior for the Duffing-van der Pol (DVP) oscillator is investigated both analytically and numerically. The critical curves separating the chaotic and non-chaotic regions are obtained. The chaotic feature on the system parameters are discussed in detail. The conditions for subharmonic bifurcations are also obtained. Numerical results are given, which verify the analytical ones.

Keywords Chaotic behavior, subharmonic bifurcations, Duffing-van der Pol oscillator, Melnikov function.

MSC(2010) 34C28.

1. Introduction

The Duffing oscillator is a non-linear differential equation used to model certain damped and driven oscillators. The equation is given by

$$\frac{d^2x}{dt^2} + \delta \frac{dx}{dt} + \alpha x + \beta x^3 = \gamma \cos(\omega t).$$

The equation describes the motion of a damped oscillator with a more complicated potential than in simple harmonic motion (which corresponds to the case $\beta = \delta = 0$); in physical terms, it models, for example, a spring pendulum whose spring's stiffness does not exactly obey Hooke's law.

In dynamics, the van der Pol (VDP) oscillator is a non-conservative oscillator with non-linear damping. It evolves in time according to the second-order differential equation:

$$\frac{d^2x}{dt^2} - \mu_0(1 - x^2) \frac{dx}{dt} + x = 0.$$

The two classical nonlinear systems, the Duffing oscillator and the VDP oscillator can describe many kinds of practical systems. They have been extensively

[†]the corresponding author.

Email address: Lchzxz3@126.com(H. Li), malilin@126.com(L. Ma), wenjingzhu122@163.com(W. Zhu)

¹Department of Mathematics, Jiujiang University, Jiujiang, Jiangxi 332005, China

²Information Technology Center, Jiujiang University, Jiujiang, Jiangxi 332005, China

³Department of Mathematics, China Jiliang University, Hangzhou, Zhejiang 310018, China

*The authors were supported by National Natural Science Foundation of China (11401274, 11661046).

investigated [1, 9, 12, 16]. As the combination of these two classical nonlinear systems, the DVP oscillator as a model of mechanics can be applied in many fields, such as physics, engineering, electronics, biology, neurology and many other disciplines.

The mathematical expression of the DVP oscillator is assumed in the form of the second-order non-autonomous differential equation

$$\frac{d^2x}{dt^2} - \mu_0(1 - x^2)\frac{dx}{dt} + \frac{dV(x)}{dx} = g(f_0, \omega, t), \quad (1.1)$$

where x stands for the displacement from the equilibrium position, f_0 is the forcing strength and $\mu_0 > 0$ is a damping parameter of the system. $g(f_0, \omega, t) = f_0 \cos(\omega t)$ represents the periodic driving function of time with period $T = \frac{2\pi}{\omega}$, ω being the angular frequency of the driving force. $V(x)$ is the potential approximated by a finite Taylor series. The DVP oscillator belongs to the category of three-dimensional dynamical system with continuous time and can be expressed in the strict feed-back form. System (1.1) is a generalization of the classic DVP oscillator equation. It can be considered in at least three physically interesting situations, wherein the potential

$$V(x) = -\alpha \frac{x^2}{2} + \beta \frac{x^4}{4} \quad (1.2)$$

is a (i) single-well ($\alpha < 0, \beta > 0$), (ii) double-well ($\alpha > 0, \beta > 0$) or (iii) double-hump ($\alpha < 0, \beta < 0$). Each of the above three cases has become a classic central model describing inherently nonlinear phenomenon exhibiting rich and baffling varieties of regular and chaotic motions.

DVP oscillator as a model of mechanics can be applied in many fields and many researches on DVP oscillator have been done. Ravisankar et al. [15] investigated the occurrence of horseshoe chaos in three different asymmetric DVP oscillators driven by a narrow-band frequency modulated force. Njah and Vincent [14] presented chaos synchronization between single and double wells DVP oscillators with potential based on the active control technique. Wang and Li [18] analyzed the nonlinear dynamical characteristics of the DVP oscillator subject to both external and parametric excitations with time delayed feedback control. Leung et al. [7] investigated the damping characteristics of two DVP oscillators having damping terms described by fractional derivative and time delay respectively. By the residue harmonic method, Leung et al. [8] investigated periodic bifurcation of DVP oscillators having fractional derivatives and time delay. Chen and Jiang [2] studied the periodic solution of the DVP oscillator by homotopy perturbation method. The nonlinear dynamics of a DVP oscillator under linear-plus-nonlinear state feedback control with a time delay are investigated by means of the averaging method and Taylor expansion [13].

In this present paper, we consider only the double-well ($\alpha > 0, \beta > 0$) and the double-hump ($\alpha < 0, \beta < 0$) cases of the following the DVP oscillator

$$\frac{d^2x}{dt^2} - \mu_0(1 - x^2)\frac{dx}{dt} - \alpha x + \beta x^3 = f_0 \cos(\omega t). \quad (1.3)$$

Assume the damping and excitation terms μ_0, f_0 are small, denoting them as $\epsilon\mu, \epsilon f$, where ϵ is a small parameter, then Eq. (1.3) can be written as the following planar system

$$\begin{cases} x' = y, \\ y' = \alpha x - \beta x^3 + \epsilon\mu(1 - x^2)y + \epsilon f \cos(\omega\xi) \end{cases} \quad (1.4)$$

where “ \prime ” is the derivative with respect to ξ .

The phase portraits of the unperturbed double-well and double-hump DVP oscillator ($\epsilon = 0$) are shown in Figure 1 and Figure 4. The parameter representations of homoclinic orbits, heteroclinic orbits and all periodic orbits of the unperturbed system can be calculated in terms of hyperbolic and elliptic functions, so that the Melnikov method can be used and all explicit bifurcation conditions on parameter space can be obtained [6, 10, 11]. The chaotic motions of the two cases are studied analytically with the Melnikov method. The critical curves separating the chaotic and non-chaotic regions are drawn. Associated phase portraits are numerically computed, which verify the analytical results. The subharmonic bifurcations are also investigated.

The paper is organized as follows. In Section 2, we present all parametric representations of phase orbits for the unperturbed system of (1.4) and discuss the chaotic behavior of Eq. (1.4) by calculating the Melnikov integrals. In Section 3, we give the conditions for subharmonic bifurcations of the DVP oscillator (1.4). Numerical results are given in Section 4.

2. Chaotic motions of the system

2.1. The double-well case ($\alpha > 0, \beta > 0$)

Using the transformations

$$x = p\sqrt{\frac{\alpha}{\beta}}, \quad \xi = \sqrt{\frac{1}{\alpha}}t, \tag{2.1}$$

then Eq. (1.4) can be written as

$$\begin{cases} p' = q, \\ q' = p - p^3 + \epsilon \frac{\mu}{\sqrt{\alpha}}(1 - \frac{\alpha}{\beta}p^2)q + \epsilon \frac{f}{\alpha} \sqrt{\frac{\beta}{\alpha}} \cos(\frac{\omega}{\alpha}t), \end{cases} \tag{2.2}$$

where “ \prime ” is the derivative with respect to t . The unperturbed system ($\epsilon = 0$) has the Hamiltonian

$$H(p, q) = \frac{1}{2}q^2 - \frac{1}{2}p^2 + \frac{1}{4}p^4 = h. \tag{2.3}$$

System (2.3) has three equilibrium points, $(p, q) = (\pm 1, 0)$ are all centers, $(p, q) = (0, 0)$ is a saddle point. When $h = 0$, there exist homoclinic orbits connecting $(0, 0)$ to itself with the expressions

$$(p_{hom}(t), q_{hom}(t)) = (\pm\sqrt{2} \sec h(t), \mp\sqrt{2} \sec h(t) \tan h(t)). \tag{2.4}$$

When $h > 0$, there exist closed periodic orbits around the homoclinic orbits (2.4) with the expressions

$$\begin{aligned} (p_k(t), q_k(t)) = & \left(\frac{\sqrt{2}k}{\sqrt{2k^2 - 1}} \operatorname{cn}\left(\sqrt{\frac{1}{2k^2 - 1}}t, k\right), \right. \\ & \left. \frac{-\sqrt{2}k}{2k^2 - 1} \operatorname{sn}\left(\sqrt{\frac{1}{2k^2 - 1}}t, k\right) \operatorname{dn}\left(\sqrt{\frac{1}{2k^2 - 1}}t, k\right) \right), \end{aligned} \tag{2.5}$$

and $\frac{1}{\sqrt{2}} < k < 1$ is the modulus of the Jacobi elliptic functions. The period of the closed orbit is $T_k = 4K(k)\sqrt{2k^2 - 1}$. When $-\frac{1}{4} < h < 0$, there exist closed periodic orbits around $(\pm 1, 0)$ with the expressions

$$\begin{aligned} (p_k(t), q_k(t)) = & \left(\sqrt{\frac{2}{2-k^2}} \operatorname{dn}\left(\sqrt{\frac{1}{2-k^2}}t, k\right), \right. \\ & \left. - \frac{\sqrt{2}k^2}{2-k^2} \operatorname{sn}\left(\sqrt{\frac{1}{2-k^2}}t, k\right) \operatorname{cn}\left(\sqrt{\frac{1}{2-k^2}}t, k\right) \right), \end{aligned} \quad (2.6)$$

where “sn, cn, dn” are Jacobi elliptic functions, and $0 < k < 1$ is the modulus of the Jacobi elliptic functions. The period of the closed orbit is $T_k = 2K(k)\sqrt{2-k^2}$, where $K(k)$ is the complete elliptic integral of the first kind. The phase portrait of the unperturbed double-well ($\alpha > 0, \beta > 0$) DVP oscillator is shown in Figure 1.

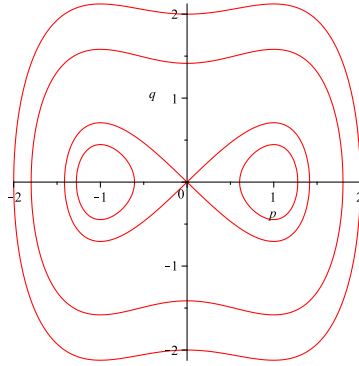


Figure 1. Phase portrait of the unperturbed double-well DVP oscillator.

By using Ref. [17], the Melnikov integral computed along the homoclinic orbit (2.4) is given by

$$\begin{aligned} M^\pm(t_0) &= \int_{-\infty}^{+\infty} q_{hom} \left(\frac{f}{\alpha} \sqrt{\frac{\beta}{\alpha}} \cos\left(\frac{\omega}{\sqrt{\alpha}}(t+t_0)\right) + \frac{\mu}{\sqrt{\alpha}} \left(1 - \frac{\alpha}{\beta} p_{hom}^2\right) q_{hom} \right) dt \\ &= \mp \int_{-\infty}^{+\infty} \frac{\sqrt{2}f}{\alpha} \sqrt{\frac{\beta}{\alpha}} \sec h(t) \tan h(t) \cos\left(\frac{\omega}{\sqrt{\alpha}}(t+t_0)\right) dt \\ &\quad + \int_{-\infty}^{+\infty} \frac{2\mu}{\sqrt{\alpha}} \left(1 - \frac{2\alpha}{\beta} \sec^2 h(t)\right) \sec h^2(t) \tan h^2(t) dt. \end{aligned} \quad (2.7)$$

Further we see from (2.7) that

$$M^\pm(t_0) = I_0 \mu \pm I_1 f \sin\left(\frac{\omega}{\sqrt{\alpha}} t_0\right), \quad (2.8)$$

where $I_0 = \frac{2}{\sqrt{\alpha}} \left(\frac{2}{3} - \frac{8}{15} \frac{\alpha}{\beta}\right)$, $I_1 = \frac{\sqrt{2}\beta\pi\omega}{\alpha^2} \frac{1}{\cosh\left(\frac{\pi\omega}{2\sqrt{\alpha}}\right)}$.

Clearly, $M^\pm(t_0)$ is an oscillating function with respect to t_0 , i.e., there exist simple zeros of $M^\pm(t_0)$ for all $|\frac{t_0}{f}| > |\frac{\mu}{f}|$. It means that the stable and unstable manifolds of the periodic orbits intersect transversely yielding small horseshoes on the appropriate energy manifold.

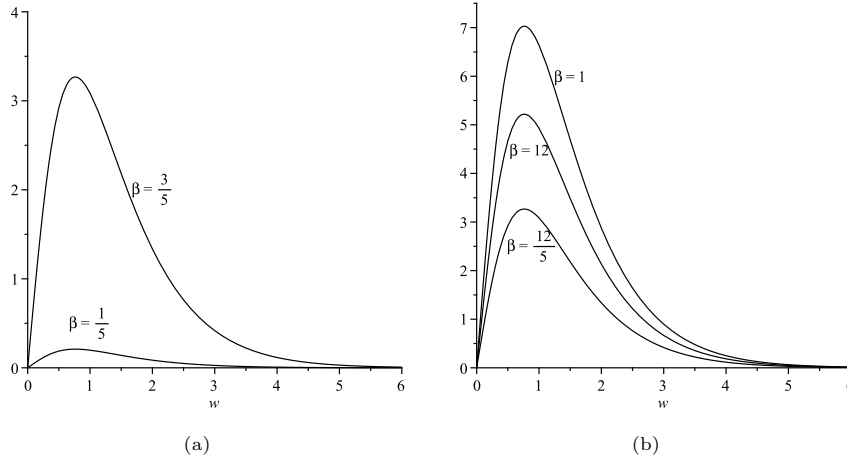


Figure 2. The critical curves for chaotic motions of system (2.2) in the case of $\alpha = 1$.

For $\frac{\alpha}{\beta} < \frac{5}{4}$, the critical value $Z = \frac{I_1}{I_0}$, when $|\frac{w}{f}| < Z$, chaotic motions take place, when $|\frac{w}{f}| > Z$, chaotic motions don't take place. When α is fixed,

$$\frac{dZ}{d\beta} = \frac{\pi\omega}{\alpha\sqrt{2\alpha\beta}} \left(\frac{1}{3} - \frac{4\alpha}{5\beta}\right) \left(\frac{2}{3} - \frac{8\alpha}{15\beta}\right)^{-2} \sec h \frac{\pi\omega}{2\sqrt{\alpha}},$$

we have $\frac{dZ}{d\beta} > 0$ for $0 < \frac{\alpha}{\beta} < \frac{5}{12}$, $\frac{dZ}{d\beta} < 0$ for $\frac{5}{12} < \frac{\alpha}{\beta} < \frac{5}{4}$. Letting $\alpha = 1$, for different value of β ($\frac{\alpha}{\beta} < \frac{5}{4}$), we get the critical curves separating the chaotic regions (below) and non-chaotic regions (above) as in Figure 2(a). When β is fixed,

$$\frac{dZ}{d\alpha} = \frac{\sqrt{2\beta}\pi\omega \sec h \frac{\pi\omega}{2\sqrt{\alpha}}}{2\alpha^{\frac{3}{2}} \left(\frac{2}{3} - \frac{8\alpha}{15\beta}\right)} \left(\frac{4}{5\beta - 4\alpha} - \frac{3}{2\alpha} + \frac{\pi\omega}{4\alpha^{\frac{3}{2}}} \tan h \frac{\pi\omega}{2\sqrt{\alpha}}\right).$$

So, when ω is small, $\frac{dZ}{d\alpha} < 0$ for $0 < \frac{\alpha}{\beta} < \frac{3}{4}$, but when ω crosses a critical value, $\frac{dZ}{d\alpha} > 0$. For $\frac{3}{4} < \frac{\alpha}{\beta} < \frac{5}{4}$, we have $\frac{dZ}{d\alpha} > 0$. Letting $\beta = 1$, for different value of α ($\frac{\alpha}{\beta} < \frac{5}{4}$), we get the critical curves as in Figure 3(a).

For $\frac{\alpha}{\beta} > \frac{5}{4}$, the critical value $Z = -\frac{I_1}{I_0}$. When α is fixed,

$$\frac{dZ}{d\beta} = -\frac{\pi\omega}{\alpha\sqrt{2\alpha\beta}} \left(\frac{1}{3} - \frac{4\alpha}{5\beta}\right) \left(\frac{2}{3} - \frac{8\alpha}{15\beta}\right)^{-2} \sec h \frac{\pi\omega}{2\sqrt{\alpha}} > 0.$$

Letting $\alpha = 1$, for different value of β ($\frac{\alpha}{\beta} > \frac{5}{4}$), we get the critical curves as in Figure 2(b). When β is fixed,

$$\frac{dZ}{d\alpha} = -\frac{\sqrt{2\beta}\pi\omega \sec h \frac{\pi\omega}{2\sqrt{\alpha}}}{2\alpha^{\frac{3}{2}} \left(\frac{2}{3} - \frac{8\alpha}{15\beta}\right)} \left(\frac{4}{5\beta - 4\alpha} - \frac{3}{2\alpha} + \frac{\pi\omega}{4\alpha^{\frac{3}{2}}} \tan h \frac{\pi\omega}{2\sqrt{\alpha}}\right),$$

we have $\frac{dZ}{d\alpha} < 0$ when ω is small, but when ω crosses a critical value, $\frac{dZ}{d\alpha} > 0$. Letting $\beta = 1$, for different value of α ($\frac{\alpha}{\beta} > \frac{5}{4}$), we get the critical curves as in Figure 3(b).

Thus, we can obtain the following theorem:

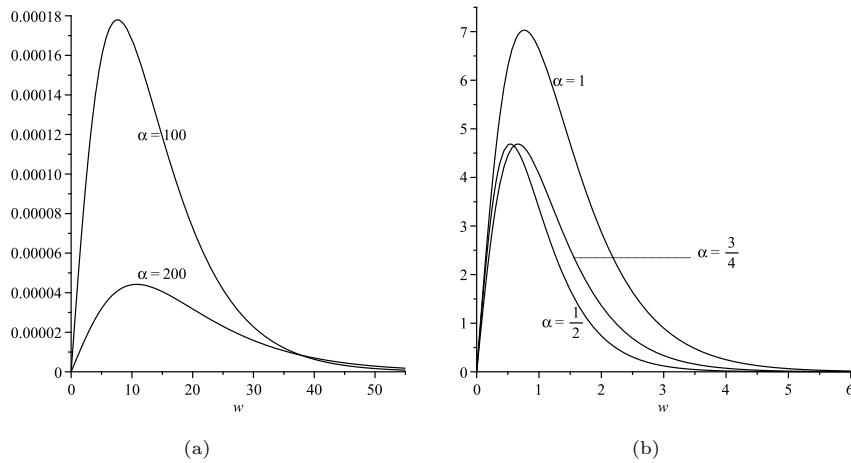


Figure 3. The critical curves for chaotic motions of system (2.2) in the case of $\beta = 1$.

Theorem 2.1. For the double-well case ($\alpha > 0$, $\beta > 0$), the critical curves of systems (2.2) have the classical bell shape, this means that, with the excitations possessing sufficiently small or very large periods, the systems are not chaotically excited.

(1) When α is fixed, if $0 < \frac{\alpha}{\beta} < \frac{5}{12}$ or $\frac{\alpha}{\beta} > \frac{5}{4}$, the larger values of β , the larger critical values for chaotic motions, and if $\frac{5}{12} < \frac{\alpha}{\beta} < \frac{5}{4}$, the larger values of β , the smaller critical values for chaotic motions.

(2) When β is fixed, if $\frac{3}{4} < \frac{\alpha}{\beta} < \frac{5}{4}$, the larger values of α , the larger critical values for chaotic motions. If $0 < \frac{\alpha}{\beta} < \frac{3}{4}$ or $\frac{\alpha}{\beta} > \frac{5}{4}$, the larger values of α , the smaller critical values for chaotic motions for the case of small values of ω , but when ω crosses a critical value, the case is opposite, so for the case of large values of ω , the critical value for chaotic motions increases as α increases.

2.2. The double-hump case ($\alpha < 0$, $\beta < 0$)

Using the transformations

$$x = p\sqrt{\frac{\alpha}{\beta}}, \quad \xi = \sqrt{-\frac{1}{\alpha}}t. \quad (2.9)$$

Then Eq. (1.4) can be written as

$$\begin{cases} p' = q, \\ q' = -p + p^3 + \epsilon \frac{\mu}{\sqrt{-\alpha}}(1 - \frac{\alpha}{\beta}p^2)q - \epsilon \frac{f}{\alpha} \sqrt{\frac{\beta}{\alpha}} \cos(\frac{\omega}{\sqrt{-\alpha}}\xi), \end{cases} \quad (2.10)$$

where “ \prime ” is the derivative with respect to t . The unperturbed system ($\epsilon = 0$) has the Hamiltonian

$$H(p, q) = \frac{1}{2}q^2 + \frac{1}{2}p^2 - \frac{1}{4}p^4 = h. \quad (2.11)$$

System (2.11) has three equilibrium points, $(p, q) = (\pm 1, 0)$ are saddle points, $(p, q) = (0, 0)$ is a center. When $h = \frac{1}{4}$, there exist exist heteroclinic orbits connecting $(\pm 1, 0)$ with the expressions

$$(p_{het}(t), q_{het}(t)) = (\pm \tan h(\frac{\sqrt{2}}{2}t), \pm \frac{\sqrt{2}}{2} \sec h^2(\frac{\sqrt{2}}{2}t)). \tag{2.12}$$

When $0 < h < \frac{1}{4}$, there exist closed periodic orbits around $(0, 0)$ with the expressions

$$(p_k(t), q_k(t)) = (\frac{\sqrt{2}k}{\sqrt{1+k^2}} \operatorname{sn}(\frac{t}{\sqrt{1+k^2}}, k), \frac{\sqrt{2}k}{1+k^2} \operatorname{cn}(\frac{t}{\sqrt{1+k^2}}, k) \operatorname{dn}(\frac{t}{\sqrt{1+k^2}}, k)), \tag{2.13}$$

and $0 < k < 1$ is the modulus of the Jacobi elliptic functions. The period of the closed orbit is $T_k = 4K(k)\sqrt{1+k^2}$. The phase portrait of the unperturbed double-hump $(\alpha < 0, \beta < 0)$ DVP oscillator is shown in Figure 4.

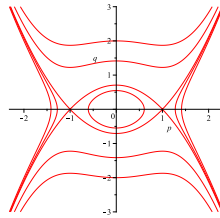


Figure 4. Phase portrait of the unperturbed double-hump DVP oscillator.

The Melnikov integral computed along the heteroclinic orbits (2.12) is given by

$$\begin{aligned} M^\pm(t_0) &= \int_{-\infty}^{+\infty} q_{het}(\frac{f}{-\alpha} \sqrt{\frac{\beta}{\alpha}} \cos(\frac{\omega}{\sqrt{-\alpha}}(t+t_0)) + \frac{\mu}{\sqrt{-\alpha}}(1 - \frac{\alpha}{\beta} p_{het}^2) q_{het}) dt \\ &= \pm \int_{-\infty}^{+\infty} \frac{\sqrt{2}f}{-2\alpha} \sqrt{\frac{\beta}{\alpha}} \sec h^2(\frac{\sqrt{2}}{2}t) \cos(\frac{\omega}{\sqrt{-\alpha}}(t+t_0)) dt \\ &\quad + \int_{-\infty}^{+\infty} \frac{\mu}{2\sqrt{-\alpha}}(1 - \frac{\alpha}{\beta} \tan h^2(\frac{\sqrt{2}}{2}t)) \sec h^4(\frac{\sqrt{2}}{2}t) dt. \end{aligned} \tag{2.14}$$

Further we see from (2.14) that

$$M^\pm(t_0) = I_0\mu \pm I_1f \cos(\frac{\omega}{\sqrt{-\alpha}}t_0), \tag{2.15}$$

where $I_0 = \frac{2\sqrt{2}}{3\sqrt{-\alpha}}(1 - \frac{\alpha}{5\beta})$, $I_1 = \frac{\sqrt{-2\beta}\pi\omega}{\alpha^2} \frac{1}{\sin h(\frac{\pi\omega}{\sqrt{-2\alpha}})}$.

Clearly, $M^\pm(t_0)$ is an oscillating function with respect to t_0 , i.e., there exist simple zeros of $M^\pm(t_0)$ for all $|\frac{I_1}{I_0}| > |\frac{\mu}{f}|$. It means that the stable and unstable manifolds of the periodic orbits intersect transversely yielding smale horseshoes on the appropriate energy manifold. Thus, we have the following conclusion.

For $\frac{\alpha}{\beta} < 5$, the critical value $Z = \frac{I_1}{I_0}$, when $|\frac{\mu}{f}| < Z$, chaotic motions take place, when $|\frac{\mu}{f}| > Z$, chaotic motions don't take place. When α is fixed,

$$\frac{dZ}{d\beta} = \frac{3\pi\omega}{-2\alpha} \sqrt{\frac{\alpha}{\beta}} (\frac{1}{2\alpha} - \frac{1}{5\beta - \alpha})(1 - \frac{1}{5} \frac{\alpha}{\beta})^{-1} \operatorname{csc} h \frac{\pi\omega}{\sqrt{-2\alpha}},$$

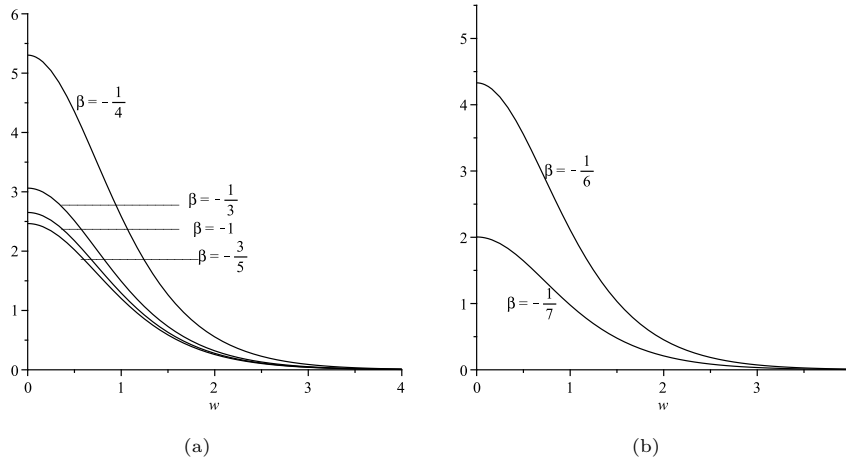


Figure 5. The critical curves for chaotic motions of system (2.10) in the case of $\alpha = -1$.

we have $\frac{dZ}{d\beta} < 0$ for $0 < \frac{\alpha}{\beta} < \frac{5}{3}$, $\frac{dZ}{d\beta} > 0$ for $\frac{5}{3} < \frac{\alpha}{\beta} < 5$. Letting $\alpha = -1$, for different value of β ($\frac{\alpha}{\beta} < 5$), we get the critical curves separating the chaotic regions (below) and non-chaotic regions (above) as in Figure 5(a). When β is fixed,

$$\frac{dZ}{d\alpha} = \frac{3\pi\omega \csc h \frac{\pi\omega}{\sqrt{-2\alpha}}}{2\alpha^2(1 - \frac{1}{5}\frac{\alpha}{\beta})} \sqrt{\frac{\beta}{\alpha}} \left(\frac{3}{2} - \frac{\alpha}{5\beta - \alpha} - \frac{3\pi\omega}{8\sqrt{-2\alpha}} \cot h \frac{\pi\omega}{\sqrt{-2\alpha}} \right).$$

So, when ω is small, $\frac{dZ}{d\alpha} > 0$ for $0 < \frac{\alpha}{\beta} < \frac{35}{17}$, but when ω crosses a critical value, $\frac{dZ}{d\alpha} < 0$. For $\frac{35}{17} < \frac{\alpha}{\beta} < 5$, we have $\frac{dZ}{d\alpha} < 0$. Letting $\beta = -1$, for different value of α ($\frac{\alpha}{\beta} < 5$), we get the critical curves as in Figure 6(a).

For $\frac{\alpha}{\beta} > 5$, the critical value $Z = -\frac{1}{I_0}$. When α is fixed,

$$\frac{dZ}{d\beta} = \frac{3\pi\omega}{2\alpha} \sqrt{\frac{\alpha}{\beta}} \left(\frac{1}{2\alpha} - \frac{1}{5\beta - \alpha} \right) \left(1 - \frac{1}{5}\frac{\alpha}{\beta} \right)^{-1} \csc h \frac{\pi\omega}{\sqrt{-2\alpha}} < 0.$$

Letting $\alpha = -1$, for different value of β ($\frac{\alpha}{\beta} > \frac{5}{4}$), we get the critical curves as in Figure 5(b). When β is fixed,

$$\frac{dZ}{d\alpha} = -\frac{3\pi\omega \csc h \frac{\pi\omega}{\sqrt{-2\alpha}}}{2\alpha^2(1 - \frac{1}{5}\frac{\alpha}{\beta})} \sqrt{\frac{\beta}{\alpha}} \left(\frac{3}{2} - \frac{\alpha}{5\beta - \alpha} - \frac{3\pi\omega}{8\sqrt{-2\alpha}} \cot h \frac{\pi\omega}{\sqrt{-2\alpha}} \right),$$

we have $\frac{dZ}{d\alpha} > 0$ when ω is small, but when ω crosses a critical value, $\frac{dZ}{d\alpha} < 0$. Letting $\beta = -1$, for different value of α ($\frac{\alpha}{\beta} > \frac{5}{4}$), we get the critical curves as in Figure 6(b).

Thus, we can obtain the following theorem:

Theorem 2.2. For the double-hump case ($\alpha < 0, \beta < 0$), the critical curves of systems (2.10) decreases to zero as ω increases from zero.

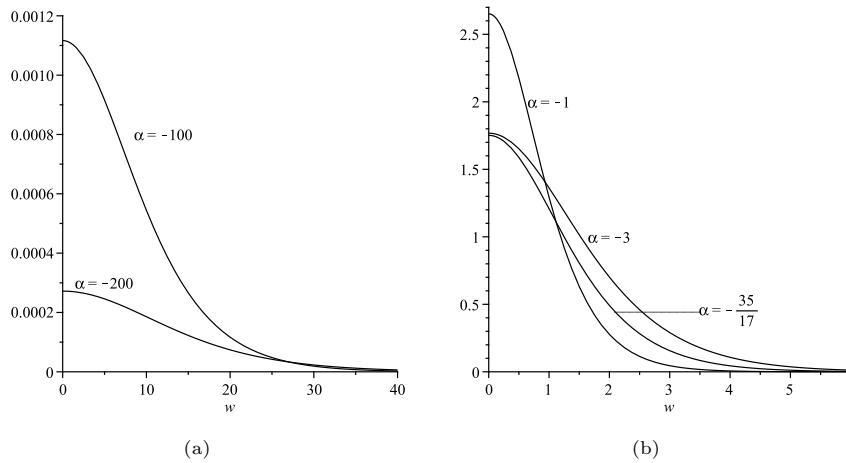


Figure 6. The critical curves for chaotic motions of system (2.10) in the case of $\beta = -1$.

(1) When α is fixed, if $0 < \frac{\alpha}{\beta} < \frac{5}{3}$ or $\frac{\alpha}{\beta} > 5$, the larger values of β , the smaller critical values for chaotic motions, and if $\frac{5}{3} < \frac{\alpha}{\beta} < 5$, the larger values of β , the larger critical values for chaotic motions.

(2) When β is fixed, if $\frac{35}{17} < \frac{\alpha}{\beta} < 5$, the larger values of α , the smaller critical values for chaotic motions. If $0 < \frac{\alpha}{\beta} < \frac{35}{17}$ or $\frac{\alpha}{\beta} > 5$, the larger values of α , the larger critical values for chaotic motions for the case of small values of ω , but when ω crosses a critical value, the case is opposite, so for the case of large values of ω , the critical value for chaotic motions decreases as α increases.

3. Subharmonic bifurcations of the system (1.4)

Consider a planar near-Hamiltonian system which has the

$$x' = f(x) + \epsilon g(t, x), \tag{3.1}$$

where $(x, \epsilon) \in \mathbb{R}^2 \times \mathbb{R}$, g is a C^2 function with period T in t , and f satisfies

$$f(x) = JDH(x), J = \begin{pmatrix} 0 & -1 \\ -1 & 0 \end{pmatrix}$$

for a C^3 function $H(x)$.

When $\epsilon = 0$, suppose there exist an open interval J such that (3.1) has a family of closed orbits $L_h : x = q(t, h), 0 \leq t \leq T(h), h \in J$ satisfying $H(q(t, h)) \equiv h$. Here $T(h)$ denotes the period of L_h .

We consider the existence of subharmonic solution of system (3.1) near L_h . We will introduce new coordinates around L_h by using its time-parameter representation. From [3, 4] we have the following lemma.

Lemma 3.1. *The transformation of the variables*

$$x = q\left(\frac{T(h)}{2\pi}\theta, h\right) \equiv G(\theta, h) \tag{3.2}$$

carries (3.1) into the 2π -periodic system

$$\begin{cases} h' = \epsilon f(G(\theta, h)) \wedge g(t, G(\theta, h), \epsilon), \\ \theta' = \Omega(h) - \epsilon \Omega(h) D_h G(\theta, h) \wedge g(t, G(\theta, h), \epsilon), \end{cases} \tag{3.3}$$

where $\Omega(h) = 2\pi/T(h)$, $a \wedge b = a_1b_2 - a_2b_1$.

To consider the subharmonic solutions of system (3.1) by Eq.(3.3) , we suppose there exists $h_0 \in J$, such that

$$\frac{T(h_0)}{T} = \frac{m}{n}, \tag{3.4}$$

with m and n are natural numbers, $(m, n) = 1$. About the existence of periodic solutions near the periodic orbit L_{h_0} , we have lemma 3.2 from [5].

The m th subharmonic Melnikov function of system (3.1) is

$$M^{m/n}(t_0) = \int_0^{mT} DH(q(t, h_0))g(t - t_0, q(t, h_0))dt. \tag{3.5}$$

Lemma 3.2. *Suppose Eq. (3.4) is satisfied and $\Omega'(h_0) \neq 0$. If there exists $t_0^* \in [0, T]$ such that*

$$M^{m/n}(t_0^*) = 0, \quad (M^{m/n})'(t_0^*) \neq 0,$$

then for sufficiently small $\epsilon \neq 0$, the periodic orbit L_{h_0} of the system (3.1) generate a subharmonic solution of order m

$$x(\epsilon, t) = q(t + t_0^*, h_0) + O(\epsilon).$$

3.1. The double-well case ($\alpha > 0, \beta > 0$)

It can be computed that the subharmonic Melnikov function of system (2.2) along the periodic orbits (2.5) and (2.6) satisfying the resonance condition $mT = nT_k$ is

$$M^{m/n}(t_0) = \frac{\mu}{\sqrt{\alpha}} J_1 - \frac{\mu\sqrt{\alpha}}{\beta} J_2 + \frac{f}{\alpha} \sqrt{\frac{\beta}{\alpha}} \sqrt{J_3^2 + J_4^2} \sin(\theta_0 + \theta_1), \tag{3.6}$$

where

$$\begin{aligned} J_1 &= \int_0^{mT} q_k^2 dt, \quad J_2 = \int_0^{mT} p_k^2 q_k^2 dt, \quad J_3 = \int_0^{mT} q_k \cos\left(\frac{\omega}{\sqrt{\alpha}} t\right) dt, \\ J_4 &= \int_0^{mT} q_k \sin\left(\frac{\omega}{\sqrt{\alpha}} t\right) dt, \quad \theta_0 = \frac{\omega}{\sqrt{\alpha}} t_0, \quad \theta_1 = \arctan \frac{J_3}{J_4}. \end{aligned}$$

(1) $h > 0$

Substituting (2.5) into (3.6), we get

$$\begin{cases} J_1 = \frac{8n}{3(2k^2-1)^{\frac{3}{2}}} [(2k^2 - 1)E(k) + (1 - k^2)K(k)], \\ J_2 = \frac{16n}{15(2k^2-1)^{\frac{5}{2}}} [2(k^4 - k^2 + 1)E(k) - (k^4 - 3k^2 + 2)K(k)], \\ J_3 = 0, \\ J_4 = \begin{cases} \frac{-\sqrt{2}m\pi^2}{\sqrt{2k^2-1}K(k)} \operatorname{csc} h \frac{m\pi K'(k)}{2K(k)}, & n=1 \text{ and } m \text{ is odd;} \\ 0, & n=1 \text{ and } m \text{ is even.} \end{cases} \end{cases} \tag{3.7}$$

Substituting (2.5) into (2.3), we have

$$H(p_k, q_k) = \frac{k^2(1 - k^2)}{(2k^2 - 1)^2},$$

$$\Omega = \frac{2\pi}{T_k} = \frac{\pi}{2K(k)\sqrt{2k^2 - 1}}.$$

Thus,

$$\frac{\partial\Omega}{\partial h} = \frac{\pi(2k^2 - 1)^{\frac{3}{2}}}{4k^2(1 - k^2)K^2(k)} [k^2E(k) + (1 - k^2)(K(k) - E(k))] > 0.$$

When m is even, $J_3 = J_4 = 0$, the condition $(M^{m/n})'(t_0^*) \neq 0$ can not be satisfied. So subharmonic bifurcation of m (even) orders will not occur; while

$$\left| \frac{\frac{\mu}{\sqrt{\alpha}}J_1 - \frac{\mu\sqrt{\alpha}}{\beta}J_2}{\frac{f}{\alpha}\sqrt{\frac{\beta}{\alpha}}\sqrt{J_3^2 + J_4^2}} \right| < 1,$$

subharmonic bifurcation of m (odd) orders will occur.

$$(2) -\frac{1}{4} < h < 0$$

Substituting (2.6) into (3.6), we get

$$\begin{cases} J_1 = \frac{4n}{3(2-k^2)^{\frac{3}{2}}} [(2-k^2)E(k) - 2(1-k^2)K(k)], \\ J_2 = \frac{8n}{15(2-k^2)^{\frac{5}{2}}} [2(k^4 - k^2 + 1)E(k) - (k^4 - 3k^2 + 2)K(k)], \\ J_3 = 0, \\ J_4 = \frac{-\sqrt{2}m\pi^2}{\sqrt{2-k^2}K(k)} \operatorname{sech} h \frac{m\pi K'(k)}{K(k)}. \end{cases} \quad (3.8)$$

Substituting (2.6) into (2.3), we have

$$H(p_k, q_k) = \frac{(k^2 - 1)}{(2 - k^2)^2},$$

$$\Omega = \frac{2\pi}{T_k} = \frac{\pi}{K(k)\sqrt{2 - k^2}}.$$

Thus,

$$\frac{\partial\Omega}{\partial h} = \frac{\pi(2 - k^2)^{\frac{3}{2}}}{2k^4(1 - k^2)K^2(k)} [(2 - k^2)(K(k) - E(k)) - k^2K(k)] < 0$$

When

$$\left| \frac{\frac{\mu}{\sqrt{\alpha}}J_1 - \frac{\mu\sqrt{\alpha}}{\beta}J_2}{\frac{f}{\alpha}\sqrt{\frac{\beta}{\alpha}}\sqrt{J_3^2 + J_4^2}} \right| < 1,$$

subharmonic bifurcation of m orders will occur.

3.2. The double-hump case $\alpha < 0, \beta < 0$

It can be computed that the subharmonic Melnikov function of system (2.10) along the periodic orbits (2.13) satisfying the resonance condition $mT = nT_k$ is

$$M^{m/n}(t_0) = \frac{\mu}{\sqrt{-\alpha}} J_1 + \frac{\mu\sqrt{-\alpha}}{\beta} J_2 - \frac{f}{\alpha} \sqrt{\frac{\beta}{\alpha}} \sqrt{J_3^2 + J_4^2} \sin(\theta_0 + \theta_1), \tag{3.9}$$

where

$$J_1 = \int_0^{mT} q_k^2 dt, \quad J_2 = \int_0^{mT} p_k^2 q_k^2 dt, \quad J_3 = \int_0^{mT} q_k \cos\left(\frac{\omega}{\sqrt{-\alpha}} t\right) dt,$$

$$J_4 = \int_0^{mT} q_k \sin\left(\frac{\omega}{\sqrt{-\alpha}} t\right) dt, \quad \theta_0 = \frac{\omega}{\sqrt{-\alpha}} t_0, \quad \theta_1 = \arctan \frac{J_3}{J_4}.$$

Substituting (2.13) into (3.9), we get

$$\begin{cases} J_1 = \frac{8n}{3(1+k^2)^{\frac{3}{2}}} [(1+k^2)E(k) - (1-k^2)K(k)], \\ J_2 = \frac{16n}{15(1+k^2)^{\frac{3}{2}}} [2(k^4 - k^2 + 1)E(k) - (k^4 - 3k^2 + 2)K(k)], \\ J_3 = \begin{cases} \frac{\sqrt{2m\pi^2}}{\sqrt{1+k^2}K(k)} \operatorname{csc} h \frac{m\pi K'(k)}{2K(k)}, & n=1 \text{ and } m \text{ is odd;} \\ 0, & n=1 \text{ and } m \text{ is even,} \end{cases} \\ J_4 = 0. \end{cases} \tag{3.10}$$

Substituting (2.13) into (2.11), we have

$$H(p_k, q_k) = \frac{k^2}{(1+k^2)^2},$$

$$\Omega = \frac{2\pi}{T_k} = \frac{\pi}{2K(k)\sqrt{1+k^2}}.$$

Thus,

$$\frac{\partial \Omega}{\partial h} = \frac{\pi(1+k^2)^{\frac{3}{2}}}{4k^2(1-k^2)^2 K^2(k)} [2K(k) - (1+k^2)(K(k) + E(k))] < 0.$$

When m is even, $J_3 = J_4 = 0$, the condition $(M^{m/n})'(t_0^*) \neq 0$ can not be satisfied. So subharmonic bifurcation of m (even) orders will not occur; while

$$\left| \frac{\frac{\mu}{\sqrt{-\alpha}} J_1 + \frac{\mu\sqrt{-\alpha}}{\beta} J_2}{\frac{f}{\alpha} \sqrt{\frac{\beta}{\alpha}} \sqrt{J_3^2 + J_4^2}} \right| < 1,$$

subharmonic bifurcation of m (odd) orders will occur.

4. Numerical simulations

In this section, we employ numerical simulations to verify the Melnikov method in analysing the chaos of systems (1.4). In all the numerical simulations, we used

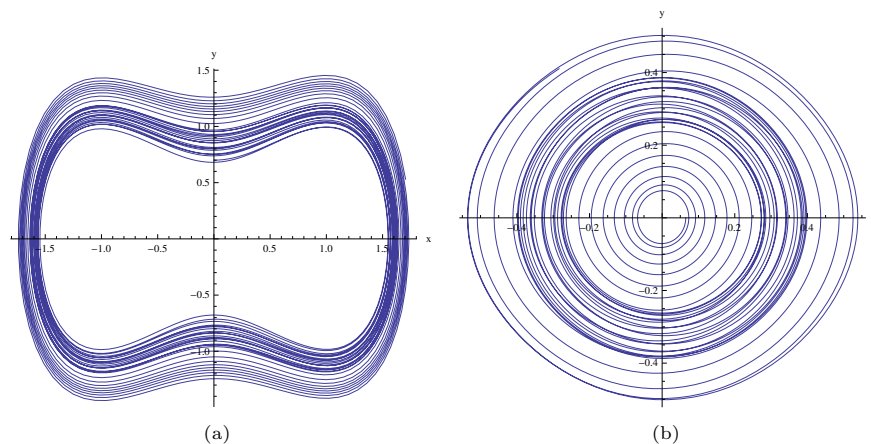


Figure 7. Phase portrait of system (1.4) for (a) $\alpha = 1, \beta = 1$ (b) $\alpha = -1, \beta = -1$.

the standard fourth-order Runge-Kutta algorithm to solve the system. Taking the system parameters $\epsilon = 0.01, \alpha = 1, \beta = 1, \mu = 1, f = 1, \omega = 1$, the initial value $(x(0), y(0)) = (0, 0.7)$, the phase portraits are shown in Figure7(a). Taking the system parameters $\epsilon = 0.01, \alpha = -1, \beta = -1, \mu = 1, f = 1, \omega = 1$, the initial value $(x(0), y(0)) = (0.065, 0)$, the phase portraits are shown in Figure7(b). Noting that for these parameters, $(|\frac{\mu}{f}|, \omega)$ is below the critical curve, i.e., it is in the chaotic region, so the system is chaotic excited, which agree with the analytical results.

References

- [1] R. Benterki and J. Llibre, *Periodic solutions of the duffing differential equation revisited via the averaging theory*, Journal of Nonlinear Modeling and Analysis, 2019, 1(1), 11–26.
- [2] A. Chen and G. Jiang, *Periodic solution of the Duffing-van der Pol oscillator by homotopy perturbation method*, International Journal of Computer Mathematics, 2010, 87, 2688–2696.
- [3] M. Han, *Bifurcations of invariant Tori and subharmonic solutions for perturbed systems*, Science in China Ser A, 1994, 11, 1325–1336.
- [4] M. Han, *Bifurcation theory of invariant Tori of planar periodic perturbed systems*, Science in China Ser A, 1996, 5, 509–519.
- [5] M. Han, *Periodic Solutions and Bifurcation Theory of Dynamical Systems*, Science Press, Beijing, 2002.
- [6] K. Kwek and J. Li, *Solitary Waves and Chaotic Behavior for a Class of Coupled Field Equations*, International Journal of Bifurcation & Chaos, 2003, 13, 643–651.
- [7] A.Y.T. Leung, Z. Guo and H. Yang, *Fractional derivative and time delay damper characteristics in Duffing-van der Pol oscillators*, Communications in Nonlinear Science and Numerical Simulation, 2013, 18, 2900–2915.
- [8] A.Y.T. Leung, H. Yang and P. Zhu, *Periodic bifurcation of Duffing-van der*

- Pol oscillators having fractional derivatives and time delay*, Communications in Nonlinear Science and Numerical Simulation, 2014, 19, 1142–1155.
- [9] J. Llibre and L. Roberto, *On the periodic solutions of a class of Duffing differential equations*, Discrete and Continuous Dynamical Systems- Series A, 2013, 33 (1), 277–282.
- [10] J. Li and Y. Zhang, *Solitary wave and chaotic behavior of traveling wave solutions for the coupled KdV equations*, Applied Mathematics & Computation, 2011, 218, 1794–1797.
- [11] J. Li, *Geometric properties and exact travelling wave solutions for the generalized Burger-Fisher equation and the Sharma-Tasso-Olver equation*, Journal of Nonlinear Modeling and Analysis, 2019, 1(1), 1–10.
- [12] S. Liang, *Exact multiplicity and stability of periodic solutions for a Duffing equation*, Mediterranean Journal of Mathematics, 2013, 10 (1), 189–199.
- [13] X. Li, J. Ji, C.H. Hanson and C. Tan, *The response of a Duffing-van der Pol oscillator under delayed feedback control*, Journal of Sound & Vibration, 2006, 291, 644–655.
- [14] A.N. Njah and U.E. Vincent, *Chaos synchronization between single and double wells Duffing-Van der Pol oscillators using active control*, Chaos, Solitons & Fractals, 2008, 37, 1356–1361.
- [15] L. Ravisankar, V. Ravichandran, V. Chinnathambi and S. Rajasekar, *Horseshoe Dynamics in an Asymmetric Duffing-Van der Pol Oscillator Driven by a Narrow-Band Frequency Modulated Force*, Chinese Journal of Physics, 2014, 52, 1041–1058.
- [16] H. Simo and P. Wofo, *Bifurcation structures of a Van der Pol oscillator subjected to nonsinusoidal periodic excitation*, International Journal of Bifurcation and Chaos in Applied Sciences and Engineering, 2012, 22(1), 125000(1–8).
- [17] S. Wiggins, *Global Bifurcations and Chaos*, Springer, New York, 1988.
- [18] Y. Wang and F. Li, *Dynamical properties of Duffing-van der Pol oscillator subject to both external and parametric excitations with time delayed feedback control*, Journal of Vibration and Control, 2015, 21, 371–387.